

From phase- to amplitude-fluctuation-driven superconductivity in systems with precursor pairing

J. Ranninger and L. Tripodi

Centre de Recherches sur les Très Basses Températures associé à l'Université Joseph Fourier, CNRS, Boîte Postale 166, 38042 Grenoble-Cédex 9, France

(Received 17 July 2002; revised manuscript received 10 September 2002; published 27 May 2003)

The change-over from phase- to amplitude-fluctuation-driven superconductivity is examined for a composite system of free electrons (fermions with concentration n_F) and localized electron pairs (hard-core bosons with concentration n_B) as a function of doping—changing the total concentration of charge carriers ($n_{\text{tot}} = n_F + 2n_B$). The coupling together of these two subsystems via a charge exchange term induces electron pairing and ultimately superconductivity in the fermionic subsystem. The difference in statistics of the two species of charge carriers has important consequences on the doping mechanism, showing an onset temperature T^* of incoherent electron pairing in the fermionic subsystem (manifest in form of a pseudogap), which steadily decreases with decreasing n_{tot} . Below T^* this electron pairing leads, in the normal phase, to electron-pair resonant states (Cooperons) with quasiparticle features which strongly depend on n_{tot} . For high concentrations, where $n_B \approx 0.5$, correlation effects between the hard-core bosons lead to itinerant Cooperons having a heavy mass m_p , but are long lived. Upon reducing the concentration of charge carriers and consequently n_B , the mass as well as the lifetime of those Cooperons is considerably reduced. As a result, for high values of n_B , a superconducting state below T^* sets in at a T_c , being controlled by the phase stiffness $D_\phi = \hbar^2 n_p / m_p$ of those Cooperons, where n_p denotes their density. Upon reducing n_{tot} , the phase stiffness steadily increases, and eventually exceeds the pairing energy $k_B T^*$. There, the Cooperons lose their well defined itinerant quasiparticle features and superconductivity gets controlled by amplitude fluctuations. The resulting phase diagram with doping is reminiscent of that of the phase fluctuation scenario for high- T_c superconductivity, except that in our scenario the determinant factors are the mass and the lifetime of the Cooperons rather than their density.

DOI: 10.1103/PhysRevB.67.174521

PACS number(s): 74.20.Mn, 74.25.-q

I. INTRODUCTION

The features which characterize classical low-temperature superconductors are the disappearance, above a certain critical temperature T_c , of a gap in the density of states (DOS) of the electrons, occurring simultaneously with the disappearance of the magnetic field expulsion (the Meissner effect) and standard Fermi-liquid behavior in the normal phase above T_c . A further characteristic is the practical impossibility to change significantly the value of T_c upon changing the concentration of charge carriers, because of T_c being largely determined by the density of states (DOS) at the Fermi level, which generally is not expected to change much with doping.

None of these features are observed in the high-temperature superconductors (HTSC's). The opening of a gap in the DOS occurs gradually, as a multitude of different experiments¹ show. This gap initially emerges in form of a pseudogap—a dip in the DOS—below a certain temperature T^* , which, depending on doping, can be much above T_c . Upon lowering the temperature and approaching T_c , this pseudogap smoothly joins the superconducting gap, as is evident from its angular variation near the Fermi surface. If the opening of the pseudogap and of the superconducting gap represent different physical manifestations of one and the same pairing mechanism, an interplay between these manifestations of electron pairing in the two phases is to be expected and is in fact observed in the form of remnant effects such as the following.

(i) A remnant of magnetic field expulsion is seen in form of a transient Meissner effect several tens of degrees above T_c , judging from the optical conductivity in the TH regime.²

This points toward long-lived diamagnetic fluctuations, which have been attributed to the presence of long-lived diffusing vortices above T_c ³, as well as to phase uncorrelated diamagnetic regions which act as precursors to the true Meissner state below T_c .⁴ Experiments, invoking Andreev reflections to interpret the enhanced tunneling conductance in the pseudogap phase,^{5,6} point toward phase uncorrelated pairing above T_c .

(ii) Remnants of local electron pairing in the c -axes optical response (orthogonal to the CuO_2 planes)⁷ in the pseudogap phase, are seen in the superconducting phase. Similarly, the c -axes component of the electronic kinetic energy is getting reduced upon entering the superconducting phase,⁸ provided the normal state exhibits pseudo gap features. The doping dependence of the c -axis penetration depth, being qualitatively similar to that of the basal plane, suggests that both are strongly influenced by the pseudogap features of the normal state.⁹ Tunneling measurements have indicated remnants of the pseudogap which continue to coexist with the superconducting gap in the superconducting phase. The latter disappears at T_c , while the former remains.¹⁰

The question whether such findings favor or not a common origin of pseudogap and of the superconducting gap is presently still being debated.^{11,12} The features in the HTSC involving the interplay of the pseudogap phase and of the superconducting phase are highly doping dependent. T^* steadily decreases with increased hole doping, while T_c shows an equally steady rise until the two approach each other. T_c then bends over and follows the descent of T^* upon further doping and approaching the optimal/overdoped re-

gime. T_c plotted as a function of the phase stiffness (determined by the square of the inverse penetration depth), involving the ratio of the density of superfluid carriers over their mass, shows a universal linear behavior.¹³

The main emphasis in this paper will be to analyze the doping dependence of T^* and T_c within a precursor pairing scenario. Very little about that doping dependence is known for such a scenario when based on single component systems, such as the negative U Hubbard model or the effective BCS Hamiltonians, extended to strong coupling. In such studies, doping is frequently introduced *ad hoc*, by assuming a doping dependent electron hopping or interelectron attraction, in view of simulating a physics close to a Mott transition. In the present paper we shall examine such doping dependent effects without making any such *ad hoc* assumptions. As we shall see, considering a mixture of itinerant electrons (fermions) and localized electron pairs (hard-core bosons) coupled together via a charge exchange term, is capable of reproducing the doping dependent features of T^* and T_c specified above. The essential new features introduced in this two-component scenario are the difference in statistics of the two components and the hard core features of the short range two-electron resonances (Cooperons) in the itinerant electron subsystem which result as a consequence of the charge exchange coupling. The variation of T_c is dictated by correlation effects of the Cooperons.

This two-component scenario has some similarity to the single-component scenarios with attractive interparticle interaction mentioned above, in as far as it can be viewed as a two-fluid picture of existing preformed pairs and unpaired electrons.¹⁴ The electron-pair resonant states which result in such a scenario have certain features which are reminiscent of localized resonance impurity states seen in the HTSC, and which arise when Cu atoms are substituted by nonmagnetic atoms such as Zn.¹⁵ Yet, the electron-pair resonant states which we are considering here have the essential potentiality of becoming itinerant and thus to lead to a superconducting phase controlled by excitations of electron pairs with finite momenta rather than pair breaking.

In Sec. II we discuss the interplay between phase and amplitude fluctuations in systems with precursor pairing, contained in the spectral properties of the Cooperon propagator. This permits us to make a connection with the phase fluctuation scenarios, which have been widely discussed in the literature. In Sec. III we briefly outline the model and the Green's function formalism which we adopt in order to treat the hard-core nature of the resonant electron pairs. In Sec. IV we present the results for the temperature variation of the density of states over a wide doping regime and analyze the doping variation of T^* . In Sec. V we explore the spectral properties of the two-particle excitations and compare the low and high density regime of the Cooperons as far as their quasiparticle properties are concerned. In Sec. VI we discuss the thermodynamics of the pseudogap phenomenon in terms of the specific heat and entropy for different doping regimes. Finally in Sec. VII we give a summary of our findings which are characteristic of precursor pairing systems, involving fermionic as well as bosonic charge carriers.

II. THE COOPERON WITHIN A PHASE FLUCTUATION SCENARIO

Based on the different experimental results mentioned in the Introduction, which clearly indicate that the physics of those HTSC is not BCS-like (over at least a wide regime of doping), it is widely agreed upon that the onset of the superconducting state in the underdoped regime in those HTSC should be controlled by phase rather than amplitude fluctuations.^{16–18} This supposes the existence of local superconducting droplets with a given phase, preexisting above T_c and evolving into a macroscopic phase locked state upon entering the superconducting state. Such a situation can be realized provided that the fluctuations of the phase of the macroscopic superconducting wave function are less costly in energy than the fluctuations of the amplitude of the electron pairs, which describe pair breaking. To within a first approximation, this so-called phase fluctuation scenario is generally described within a hydrodynamic formulation of a spatially fluctuating phase ϕ and its conjugate variable δn_s , which describes the spatial fluctuations of the superfluid particle density n_s . The corresponding effective Hamiltonian is given by

$$H = \frac{1}{2} D_\phi (\nabla \phi)^2 + \frac{1}{2\chi n_s^2} (\delta n_s)^2, \quad (1)$$

where $D_\phi = \hbar^2 (n_s / m_s)$ denotes the superfluid phase stiffness, χ the compressibility, and m_s their respective mass. The temperature which controls the phase order of such a system is given by $k_B T_\phi \approx D_\phi a$, with a being either given by the coherence length ξ for three-dimensional (3D) systems or by the interlayer distance in layered compounds such as HTSC's.

This phase fluctuation scenario is frequently discussed in conjunction with the so-called BCS-BEC cross-over phenomenon,¹⁹ where, as a function of the strength of the interparticle attraction, one passes from a BCS state at weak attraction to a Bose Einstein condensation (BEC) of tightly bound electron pairs in the limit of strong attraction. The physics for that has been widely studied on the basis of effective BCS and negative U Hubbard Hamiltonians, aiming to treat the single-particle and two-particle features on the same footing. The pseudogap in such a scenario arises from short range electron pairing, correlated over a finite time scale, comparable to the energy scale of the zero-temperature superconducting gap. According to a general theorem (due to Bogoliubov) and based on the singular behavior of the occupation number of electron pairs with small momenta which signal bound states, such electron pairing ought to survive below T_c .²⁰ A possible experimental verification for that might come from the so-called *peak-dip-hump* feature in ARPES,²¹ which shows a spectral behavior upon entering the superconducting phase, where a sharp peak (related to superconducting correlations of the low energy excitations) emerges out of the broad incoherent background, characterized by a broad hump and representing remnants of the pseudogap phase.

An attempt to formulate the problem of local pairing as a prerequisite of superconductivity was made a long time ago by generalizing the mean field BCS formalism such as to cover the regime above as well as below T_c .²² Instead of using the order parameter, the propagator for the electron pairs, also called Cooperons, is introduced and treated on the same level as the single electron propagator. Within such a formalism, and on a quite general basis, the pseudogap phase of the HTSC has been examined,²³ invoking the mutual feedback effect between the single- and the two-particle properties via the introduction of some effective gap above T_c .

A different procedure was followed by proposing a specific structure of the Cooperon propagator²⁴ of the form

$$C(\mathbf{r}, t) = C_a \exp(-r/r_0) + C_\phi \langle e^{i\phi(\mathbf{r}, t)} e^{-\phi(0,0)} \rangle, \quad (2)$$

separating amplitude from phase correlations in an additive way. The first term, representing a rather rapidly decreasing function with r , describes local pair amplitudes which are treated in a time independent fashion. The second term describes the phase correlations, which, in the low-frequency limit, are approximately expressed by $C_\phi \exp[-r/\xi(T)]$, where $\xi(T)$ denotes the temperature-dependent coherence length. Attributing that latter contribution of the Cooperon propagator to a $2D$ XY physics above the Kosterlitz-Thouless critical temperature T_{KT} , establishes a link with the phase fluctuation scenario. The doping behavior of such precursor systems as the HTSC is then monitored by parameterizing the relative weight of the coefficients C_a, C_ϕ together with the relative spatial extent of the two contributions of $C(\mathbf{r}, t)$ such that it describes the following.

(i) An underdoped regime, characterized by primarily phase fluctuation controlled onset of superconductivity with a large temperature regime for the pseudogap phase.

(ii) An optimal/overdoped regime, characterized by a gradual disappearance, upon increased doping, of the pseudogap phase and a superconducting phase, controlled by amplitude correlations.

Considering the origin of the pseudogap as being due to pair fluctuations, also called precursor pairing (not to be confused with preformed pairs), the characteristic temperature T^* below which the opening of the pseudogap occurs for such single-component scenarios with interparticle attraction, scales with the strength of that interaction.²⁵⁻²⁸ However, as far as the concentration dependence of T_c and T^* is concerned within such scenarios, it invariably shows that both T^* and T_c follow the same trend^{29,30} upon varying the number of charge carriers. This is clearly the opposite to what is found in the HTSC. Potential dimensionality changes, linked to the change-over from underdoped to overdoped materials, cannot remedy this situation either, since as far as T^* is concerned, it is determined by essentially local physics and thus independent on any dimensional aspects. As far as T_c is concerned, even upon assuming a cross-over, with reduced doping, to a Kosterlitz-Thouless critical temperature behavior in the underdoped regime, T_{KT} would still follow the same doping trend as T^* . It thus seems likely that correlation effects are indispensable in determining the doping dependence of T_c versus T^* in such precursor scenarios.

III. THE MODEL AND THE TECHNIQUE EMPLOYED

The scenario of a mixture of itinerant fermions (band electrons) and localized hard-core bosons (bound electron pairs) will be described on the basis of the so-called boson-fermion model (BFM). This model presents a paradigm for interacting electron systems where two-particle resonant states are expected to occur due to the interaction of the electrons with certain bosonic modes and where such two-particle resonant states act as precursor to a transition into a superconducting state. The underlying physics behind this model,³¹ as it was initially conceived,³² is that of electrons strongly coupled to local phonons, which act as such bosonic modes. This results in self-trapped entities, comprising the charge carriers and the surrounding clouds of bosonic excitations, in form of resonant pair states inside a system of itinerant electrons. Such a BFM scenario is not in any way restricted to electronic systems undergoing a superconducting transition but ought equally well apply to electron-hole pairing in semiconductors,³³ and low density nuclear matter with isospin singlet pairing.³⁴ Moreover, it was in a similar spirit that such a boson-fermion mixture scenario has been derived recently for (i) the Hubbard model with intermediate repulsive coupling,³⁵ (ii) the Feshbach resonance in atomic physics, controlling the strength of attraction between atoms of different hyperfine configurations by adequately tuning a magnetic field³⁶ and (iii) for entangled atoms in squeezed states in molecular Bose Einstein condensates in traps.³⁷ More generally, the BFM has been employed in attempts to bosonize an intrinsically fermionic system.³⁸

The model Hamiltonian describing the boson fermion scenario is given by

$$H_0 = (D - \mu) \sum_{i\sigma} c_{i\sigma}^+ c_{i\sigma} + (\Delta_B - 2\mu) \sum_i \left(\rho_i^z + \frac{1}{2} \right) + t \sum_{i \neq j, \sigma} c_{i\sigma}^+ c_{j\sigma} + v \sum_i (\rho_i^+ c_{i\downarrow} c_{i\uparrow} + \rho_i^- c_{i\uparrow}^+ c_{i\downarrow}^+), \quad (3)$$

where the localized hard-core bosons are represented by pseudospin-1/2 operators $[\rho_i^+, \rho_i^-, \rho_i^z]$ and the itinerant electrons by $[c_{i\sigma}, c_{i\sigma}^+]$. v denotes the strength of the onsite hybridization between the two types of charge carriers and t the hopping integral for the itinerant electrons with a band half width D . The full band width $2D$ will be used as the energy unit through out this paper. The energy level of the localized bosons is given by Δ_B and the chemical potential μ is chosen to be common to both species, such as to ensure total charge conservation $n_{\text{tot}} = n_F + 2n_B$. n_F and n_B denote the occupation number per site of the electrons (including up and down spin states) and of the hard core bosons.

The opening of the pseudogap and its temperature dependence on the basis of this model, for a fixed concentration and upon neglecting the hard-core nature of the bosons has been studied previously.³⁹⁻⁴¹ In a study based on the dynamical mean field approach,⁴² the hard-core nature of the bosons could be taken into account. But then, the itinerancy of the bosons could not be treated within such a scheme which restricted this study to purely amplitude fluctuations driven superconductivity. In the present work we shall account for

both, the hard-core nature of the bosons as well as their potentiality becoming itinerant and shall study the pseudogap characteristics as a function of total carrier concentration. The present study follows closely the previous self-consistent diagrammatic approach,³⁹ but generalizes it such as to take into account the hard-core nature of the bosons. We adopt for that purpose the diagrammatic technique which had been developed for spin systems^{43,44} (with their convention $[\rho^+, \rho^-] = \rho^z$) and for which it was shown that the usual Wick theorem had to be generalized to

$$\begin{aligned} & \langle T\{\rho_1^{\alpha_1}(\tau_1) \cdots \rho_0^-(\tau) \cdots \rho_n^{\alpha_n}(\tau_n)\} \rangle_0 \\ &= K_{01}^0(\tau - \tau_1) \langle T\{[\rho_1^{\alpha_1}, \rho_0^-]_{\tau_1} \rho_2^{\alpha_2}(\tau_2) \cdots \rho_n^{\alpha_n}(\tau_n)\} \rangle_0 \\ &+ K_{02}^0(\tau - \tau_2) \langle T\{\rho_1^{\alpha_1}(\tau_1) [\rho_2^{\alpha_2}, \rho_0^-]_{\tau_2} \cdots \rho_n^{\alpha_n}(\tau_n)\} \rangle_0 \\ &+ \dots \end{aligned} \quad (4)$$

with

$$\begin{aligned} K_{11'}(\tau - \tau') &= \delta_{11'} K^0(\tau - \tau'), \\ K^0(\tau - \tau') &= \frac{\langle T \rho^-(\tau) \rho^+(\tau') \rangle_0}{\langle \rho^z \rangle_0} \\ &= e^{-E_0(\tau - \tau')} n(x_0) \theta(\tau - \tau') \\ &+ e^{-E_0(\tau - \tau')} [1 + n(x_0)] \theta(-\tau + \tau'), \\ n(x_0) &= \frac{1}{e^{x_0} - 1}, \quad x_0 = -\beta E_0. \end{aligned} \quad (5)$$

Recursively applying this procedure of the modified Wick theorem, the remaining multi-spin correlation functions are transformed step by step into a sum of products of K_{ij}^0 multiplied with thermal averages of the type $\langle \rho_i^z \cdots \rho_n^z \rangle_0$ [evaluated with respect to the unperturbed Hamiltonian ($\Delta_B - 2\mu$) $\sum_i (\rho_i^z + \frac{1}{2})$]. These thermal averages are expressed in terms of a set of cumulants, the first few of which are given by

$$\begin{aligned} \langle \rho_1^z(\tau) \rangle &= b = -\frac{1}{2} + n_B, \\ \langle \rho_1^z(\tau) \rho_2^z(\tau) \rangle &= b^2 + b' \delta_{1,2}, \quad b^2 + b' = \frac{1}{4}, \\ \langle \rho_1^z(\tau) \rho_2^z(\tau) \rho_3^z(\tau) \rangle &= b^3 + bb'(\delta_{1,2} + \delta_{2,3} + \delta_{3,1}) + b'' \delta_{1,2} \delta_{2,3}, \\ b^3 + 3bb' + b'' &= \frac{1}{4} b \end{aligned} \quad (6)$$

Keeping only the first two cumulants b and b' gives rise to the set of diagrams, illustrated in Fig. 1, and describe the set of self-consistent equations determining the Fermion [Fig. 1(a)] and boson Green's functions [Fig. 1(b)] $G(k, \omega_n)$ and $K(q, \omega_m)$. The vertex depicted by the full square in those figures is made up of two contributions: one arising from the

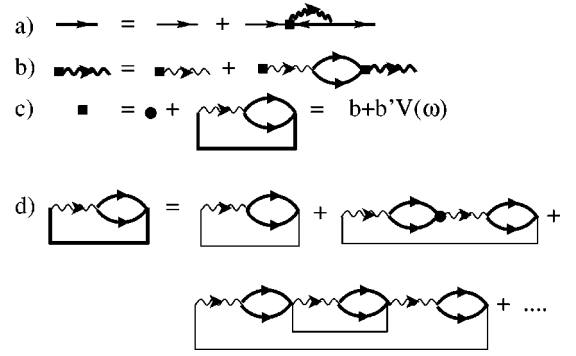


FIG. 1. Diagrammatic representation of the fermion (a), boson (b), and the vertex correlation functions (c),(d).

cumulant b and depicted by a full circle and one arising from the cumulant b' , illustrated by the second contribution to this vertex. Both those vertex contributions have to be determined self-consistently. For the contribution arising from the cumulant b it simply is $b = -1/2 + n_B$. For the contribution arising from the second cumulant, given by $b'V(\omega)$ the self-consistent equation corresponding to the set of diagrams illustrated in Fig. 1(d) has to be solved. To within this approximation of cumulants, this leads to the following set of equations:

$$\begin{aligned} G(k, \omega_n) &= \frac{1}{i\omega_n - \varepsilon_k - \Sigma(k, \omega_n)}, \\ K(q, \omega_m) &= \frac{b + b'V(\omega_m)}{i\omega_m - E_0 - [b + b'V(\omega_m)]\Pi(q, \omega_m)}, \\ G^0(k, \omega_n) &= \frac{1}{i\omega_n - \varepsilon_k}, \quad K^0(\omega_m) = \frac{b}{i\omega_m - E_0}, \\ V(\omega_m) &= V_0(\omega_m) + K_0(\omega_m) \frac{1}{N} \sum_q \Pi^2(q, \omega_m) K(q, \omega_m), \\ V_0(\omega_m) &= \frac{1}{N} \sum_q \frac{\Pi(q, \omega_m)}{i\omega_m - E_0} \end{aligned} \quad (7)$$

with $E_0 = \Delta_B - 2\mu$ and the bare electron dispersion $\varepsilon_{\mathbf{k}} = D[1 - (1/Nz) \sum_{\langle r_i \neq r_j \rangle} e^{i\mathbf{k}(r_i - r_j)}] - \mu$. The self-energies for the Fermions and hard-core bosons are given by

$$\begin{aligned} \Sigma(\mathbf{k}, \omega_n) &= -\frac{v^2}{\beta N} \sum_{\mathbf{q}, \omega_m} G(\mathbf{q} - \mathbf{k}, \omega_m - \omega_n) K(\mathbf{q}, \omega_m), \\ \Pi(\mathbf{q}, \omega_m) &= \frac{v^2}{\beta N} \sum_{\mathbf{k}, \omega_n} G(\mathbf{q} - \mathbf{k}, \omega_m - \omega_n) G(k, \omega_n). \end{aligned} \quad (8)$$

This set of equations represents a generalization of the usual self-consistent RPA equations for this BFM problem^{39,40} when restricting oneself to the lowest order approximation involving only the cumulant b . The contributions arising from higher order cumulants bring in frequency dependent vertex corrections $V(\omega)$. Keeping only the lowest

cumulant in the expression for $K(\mathbf{q}, \omega_m)$ corresponds to a boson Green's function which is identically zero in the limit of $n_B = 0.5$. Hence, close to this limit the second order cumulant expansion has to be used as a starting point. The full set of Eq. (8) (including both first and second order cumulants) was solved for a restricted set of values for temperatures and total particle concentrations and the results were compared with those obtained when keeping the lowest order cumulant only. Except for boson densities close to $n_B = 0.5$, the lowest order cumulant approximation provides the dominant contribution to the solutions of these equations. The results presented in this paper cover a boson density regime between 0 and ≈ 0.35 for which this lowest order cumulant approximation can be considered as being qualitatively correct. Upon approaching $n_B = 0.5$ [where the full set of Eq. (8) had to be dealt with] we encountered convergence problems with the iterative solution algorithm employed here which became exceedingly more important the lower the temperature was.

The Green's functions for the fermions and the hard-core bosons are defined by

$$\begin{aligned} G_{i,j}(\tau, \tau') &= -\langle T[c_{i\sigma}(\tau)c_{j\sigma}^+(\tau')] \rangle \\ &= \frac{1}{N\beta} \sum_{\mathbf{k}, n} e^{i\mathbf{k}(\mathbf{r}_i - \mathbf{r}_j) - i\omega_n(\tau - \tau')} G(\mathbf{k}, \omega_n), \\ K_{i,j}(\tau, \tau') &= \langle T[\rho_i^-(\tau)\rho_j^+(\tau')] \rangle \\ &= \frac{1}{N\beta} \sum_{\mathbf{q}, m} e^{i\mathbf{q}(\mathbf{r}_i - \mathbf{r}_j) - i\omega_m(\tau - \tau')} K(\mathbf{q}, \omega_m), \end{aligned} \quad (9)$$

where $\omega_n = \pi(2n+1)/\beta$ and $\omega_m = \pi 2m/\beta$ denote the Matsubara frequencies for fermions and bosons, respectively, n and m running over all integers from $-\infty$ to $+\infty$. The expressions for the self-energies for the fermions $\Sigma(\mathbf{k}, \omega_n)$ and for the hard-core bosons $\Pi(\mathbf{q}, \omega_m)$ differ from the standard ones for ordinary bosons by a change in sign due to the Wick theorem for hard-core bosons. The effect of the cumulants, however, corrects this sign change in the end because of the presence of the factor b in the numerator of the Bose Green's function. Fixing n_{tot} , Eqs. (7) are solved numerically on the Matsubara axes and the resulting Green's functions and self-energy functions are then analytically continued onto the real frequency axes, via the usual Padé type procedure. The Green's functions G and K are linked to the occupation numbers $n_{\mathbf{k}}^F = (2/\beta) \sum_{\omega_n} e^{-i\omega_n 0^-} G(\mathbf{k}, \omega_n)$ and $n_{\mathbf{q}}^B = (2/\beta) \sum_{\omega_m} e^{-i\omega_m 0^-} K(\mathbf{q}, \omega_m)$ for the fermions and bosons, respectively, with $n_{F,B} = (1/N) \sum_{\mathbf{k}} n_{\mathbf{k}}^{F,B}$.

As a typical example for the present study we choose the energy level of the hard-core bosons to lie in the center of the band of itinerant electrons ($\Delta_B = 1$) and assume a small value of the exchange coupling constant ($v^2 = 0.02$). Requiring the chemical potential to lie slightly below the bosonic level ($\mu \leq 0.5$), assures us that upon changing the total number of charge carriers n_{tot} from 2 to 1, we recover a situation which, as far as the density of electrons is concerned, mimics the situation encountered in HTSC over a wide doping re-

gime. We shall for that reason adopt the terminology, widely used in connection with studies on the HTSC's, and refer to the doping regime $2 \geq n_{\text{tot}} \geq n_0$ as the underdoped regime and $n_{\text{tot}} \leq n_0$ as the optimal/overdoped regime, with $n_0 \approx 1.1$ for our choice of parameters. We furthermore restrict the momentum summations over a 1D Brillouin zone with 200 k points. This is justified, since we are interested here in only very general features of the pseudogap phenomenon. If our results, have any bearing on the physics of HTSC, they should apply to regions in momentum space where the pseudogap phenomenon is most pronounced, i.e., near the so-called *hot spots* around the M points in the Brillouin zone of the basal plane. There they could describe d wave symmetry pseudogap behavior along one of its lobes along a direction $[0,0] - [0,\pi]$ and their equivalents, traversing the M points. Our results could thus possibly be compared with ARPES spectra for wave vectors along such directions in k space, as well to transport measurements along the same directions.

IV. THE DOPING AND TEMPERATURE DEPENDENCE OF THE PSEUDOGAP

We present in the following the results of the solution of the set of self-consistent equations (7), (8), together with a self-consistent determination of the lowest cumulant b , Eq. (6). This permits us to determine the electronic DOS as a function of temperature for different "doping rates," given by n_{tot} , or alternatively, by the depletion of the Fermi sea away from half filling, given by $(1 - n_F)$. In this BFM scenario, doping influences both the number of itinerant electrons n_F as well as the number of bound electron pairs n_B . This is not an unrealistic premise as far as the HTSC are concerned, since it has been experimentally established that doping does not occur exclusively in the CuO_2 planes but involves also the dielectric layers between them. This is born out by XPS studies which permit to determine the relative change with doping of the population of Cu^+ versus Cu^{++} ions.⁴⁵ Further indications that doping occurs in a multicomponent system comes from measurements of the size of the Fermi surface volume⁴⁶ which show that the universal curve for T_c as a function of doping is shifted downwards in doping as compared to its dependence on the chemical doping rate. And finally, site dependent XAFS studies⁴⁷ show that in order for the superconducting phase to materialize, doping must necessarily involve holes located outside the metallic CuO_2 planes. Further evidence for the existence of two species of different charge carriers, itinerant ones (giving rise to a Drude peak) and localized ones (giving rise to a peak in the far infrared regime), comes from reflectivity measurements.⁴⁸

Given our choice of the boson level falling in the middle of the band of itinerant electrons, fixes the Fermi level such that we have the situation of a half-filled band for $n_{\text{tot}} = 2$. Upon hole doping we move the chemical potential downwards from its value at D , which introduces holes in the electronic subsystem and at the same time diminishes n_B . This variation of n_B as function of μ is illustrated in Fig. 2 for different temperatures. The bound electron pairs, being

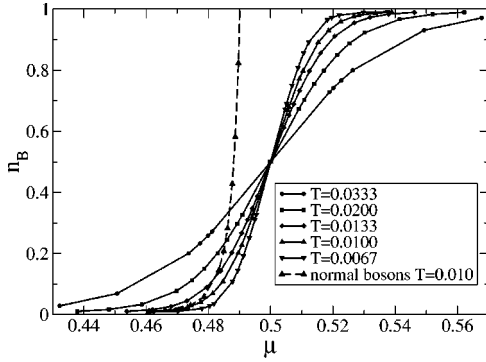


FIG. 2. Comparison of the variation of the number of normal to hard-core bosons as a function of the chemical potential for several temperatures.

hard-core bosons, lead to a fully symmetric situation for particle and hole doping for this choice of parameters. We also illustrate in this figure the variation of n_B with μ for ordinary bosons, which significantly differs from that of hard-core bosons.

In order to study the evolution of the pseudogap as a function of temperature and doping, we evaluate the spectral function of the single-particle fermionic Green's function $A_F(\mathbf{k}, \omega) = 2 \text{Im} G(\mathbf{k}, i\omega_n \rightarrow \omega + i\delta)$ which, after integrating over all wave vectors in the Brillouin zone gives us the DOS $\rho(\omega)$. In Fig. 3 we plot the evolution of the pseudogap near the chemical potential (corresponding to $\omega = 0$) as a function of temperature and for several doping concentrations $n_{\text{tot}} \approx 1.66, 1.20,$ and 0.97 . In order to determine T^* as a function of n_B and n_{tot} , respectively, we illustrate in Fig. 4 the minimum of the dip in the DOS given by $\rho_{\text{min}}(T)$, as a function of n_B for different temperatures. We then consider the relative values of this depletion of the DOS, determined by $\rho_{\text{min}}(T)/\rho_{\text{min}}(\infty)$ and cut these functions by horizontal lines, lying 4% below the saturation values of $\rho_{\text{min}}(\infty)$. [Within the lowest order cumulant approximation—putting $b' = 0$ —we would have obtained a $\rho_{\text{min}}(n_B)$ which as a function of n_B would have show an upturn upon approaching $n_B = 0.5$.] The crossing points determine the values of T^* for any particular n_{tot} and its corresponding value of n_B . T^* , representing a cross-over rather than a phase transition, thus

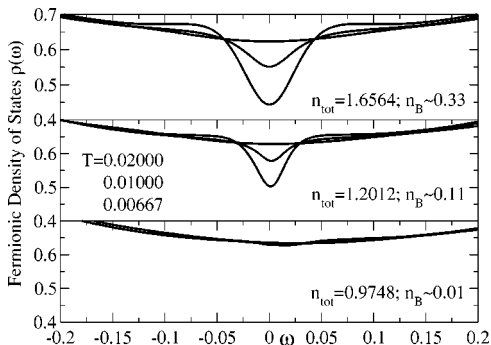


FIG. 3. Evolution of the pseudogap near the chemical potential as a function of temperature for $\Delta_B = 1$ and different doping concentrations n_{tot} .

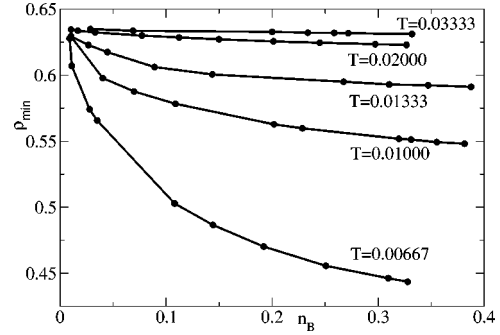


FIG. 4. Dependence of the minimum in the DOS on the concentration of hard-core bosons n_B for different temperatures and $\Delta_B = 1$.

corresponds to that temperature where the deviation from the high temperature saturated DOS close to the Fermi energy is reduced by an arbitrary but small amount, chosen here as 4%. In Fig. 5 we illustrate the variation of T^* as a function of n_{tot} as well as of $(1 - n_F)$; the latter being a measure of the deviation of the Fermion occupation from the half-filled band situation and thus of hole doping.

It is illustrative to compare this doping dependence of T^* , derived from the dip in the DOS in the normal state, with the doping dependence of the mean field critical temperature T_c^{MF} for amplitude fluctuation controlled superconductivity. That latter is characterized by the order parameters

$$x = \frac{1}{N} \sum_i \langle c_i^+ c_i^+ \rangle, \quad \rho = \frac{1}{N} \sum_i \langle \rho_i^+ + \rho_i^- \rangle \quad (10)$$

which refer to the off diagonal elements of the charge operators of the electron pairs and hard-core bosons, respectively. Solving this mean field equation problem (for details for such an analysis the reader is referred to an earlier paper⁴⁹) gives rise to a T_c^{MF} which exhibits a doping dependence which is quite similar to that of T^* (see Fig. 5), with an onset of amplitude fluctuation controlled superconductivity slightly below that temperature where electron-pair fluctuations set in. T_c^{MF} does not, of course, have the meaning of a transition temperature for the onset of superconductivity, which, as we

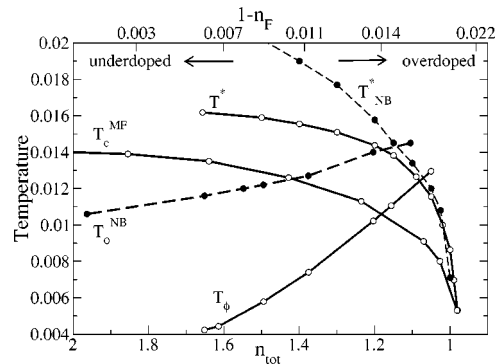


FIG. 5. Doping dependence of T^* , compared with the mean field critical temperature T_c^{MF} , and the “phase fluctuation” temperatures T_ϕ . For comparison we also illustrate this doping dependence by T_{NB}^* and T_ϕ^{NB} when treating the bosons as normal bosons.

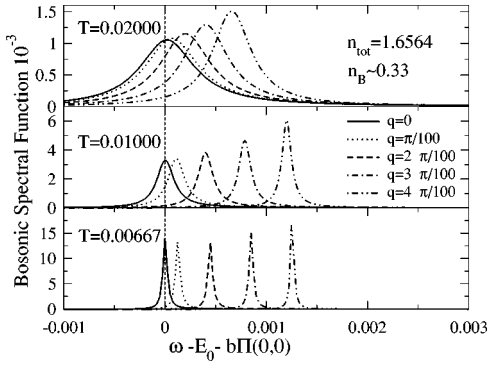


FIG. 6. Temperature evolution of the boson spectral function for the low wave vectors for the underdoped regime with $n_{\text{tot}} = 1.65$.

shall see in the next section, is induced by phase rather than amplitude fluctuations, except for the limit of low boson concentrations where T_c^{MF} and T^* smoothly join.

It is an interesting question to ask how this doping dependence of T^* changes when instead of hard-core bosons one considers normal bosons. We plot in Fig. 5 the temperature T_{NB}^* , signalling the opening of the pseudogap in that case. It shows a monotonically decreasing behavior with decreasing n_{tot} , similar to that found for hard-core bosons but does not saturate, as is the case for those latter, when approaching the fully symmetric limit $n_{\text{tot}} = 2$.

V. SPECTRAL PROPERTIES OF THE COOPERON PROPAGATOR

Let us now examine the features of the normal state which act as a precursor of the superconducting phase. As previously shown,⁴⁰ the intrinsically localized bound electron pairs (bosons), gradually acquire itinerancy as the temperature is lowered below T^* . We shall explore this behavior here as a function of doping and focus on the effect of the hard-core nature of those bosons, which has been neglected in such previous studies. The resonant electron-pair states in the fermionic subsystem, induced by the exchange with the bound electron pairs of the bosonic subsystem, are described by the spectral properties of the Cooperon propagator

$$C(\mathbf{q}, \tau) = \frac{1}{N^2} \sum_{\mathbf{k}, \mathbf{k}'} \ll c_{\mathbf{q}-\mathbf{k}\uparrow}^+(\tau) c_{\mathbf{k}\downarrow}^+(\tau); c_{\mathbf{k}'\downarrow}(0) c_{\mathbf{q}-\mathbf{k}'\uparrow}(0) \gg, \quad (11)$$

which are intimately linked to the spectral properties of the single-particle bose Green's function $K(\mathbf{q}, \omega_m)$ via the relation

$$C(\mathbf{q}, \omega_m) = \frac{1}{v^2} \Pi(\mathbf{q}, \omega_m) + \frac{1}{v^2} \Pi^2(\mathbf{q}, \omega_m) K(\mathbf{q}, \omega_m). \quad (12)$$

The thermodynamic and transport properties of our system are given by the low lying excitation spectrum of those resonant electron pairs. Their spectral properties are determined by spectral functions of the hard-core bosons, given by the second term in Eq. (12). In Figs. 6–8 we illustrate those

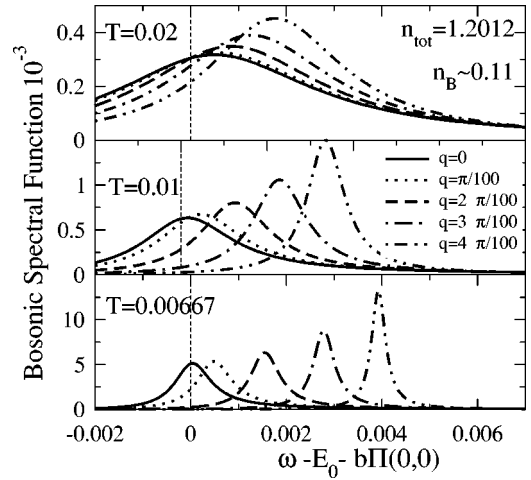


FIG. 7. Temperature evolution of the boson spectral function for the low wave vectors for the underdoped regime with $n_{\text{tot}} = 1.20$.

spectral functions for the long wavelength regime together with their evolution with temperature for three representative concentrations, which cover the entire doping regime from underdoped ($n_{\text{tot}} \approx 1.65$) with a high concentration of bosons to the optimally overdoped ($n_{\text{tot}} \approx 0.97$) with a low concentration of bosons. We find that in the underdoped regime the Cooperons are well defined propagating modes with a narrow width of the spectral function which, moreover, strongly decreases with decreasing temperature (see Figs. 6, 7). In the optimally/overdoped regime, on the contrary, the spectral functions show overdamped mode behavior (see Fig. 8). Tracing the peak position of the boson spectral function as a function of wave vector \mathbf{q} permits us to determine the mass m_p of those Cooperons. As we approach the dense limit of bosons, m_p increases sensibly, when we compare this mass for different values of doping (n_{tot}) at a fixed given temperature (see Table I). For the low doping regime where the bosons are well defined quasiparticles, their DOS shows an evolution with temperature in which the low energy part gets more and more peaked as the temperature is lowered and the peak position approaches the value $E_0 + b\Pi(0,0)$, (see Figs. 9, 10), as it should according to the Hugenholtz Pines theorem.⁵⁰

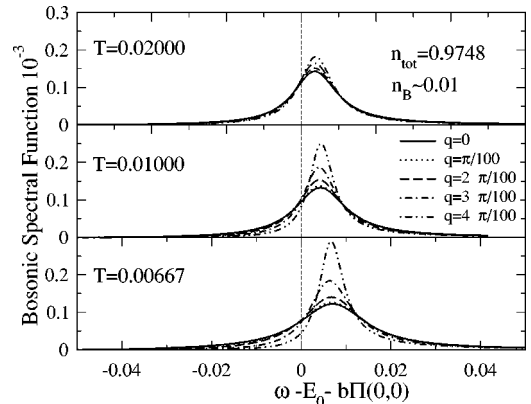


FIG. 8. Temperature evolution of the boson spectral function for the low wave vectors for the optimally overdoped regime with $n_{\text{tot}} = 0.97$.

TABLE I. Variation with doping n_{tot} of m_p (in units of $1/D$) and n_p for a fixed temperature $T=0.00667$ and the estimated resulting T_ϕ . We present in parenthesis the corresponding values when the bosons are treated as normal instead of hard-core bosons.

n_{tot}	m_p	$n_p 10^3$	T_ϕ
1.651	2.27 (1.29)	9.60 (14.9)	0.0042 (0.0116)
1.614	2.14 (1.24)	9.49 (14.5)	0.0044 (0.0117)
1.495	1.56 (1.06)	9.04 (12.9)	0.0058 (0.0112)
1.376	1.14 (0.88)	8.44 (11.2)	0.0074 (0.0127)
1.204	0.71 (0.62)	7.30 (8.71)	0.0102 (0.0140)
1.156	0.63 (0.55)	6.91 (7.98)	0.0111 (0.0145)
1.105	0.45 (0.49)	5.88 (7.10)	0.0124 (0.0145)

We next turn to the evaluation of the concentration of Cooperons, which, together with their mass will enable us to estimate the phase stiffness in that system and thus the onset temperature of superconductivity due to phase fluctuations T_ϕ . The density of Cooperons, acting as superfluid charge carriers, is contained in the combination of n_p/m_p entering the expression for the penetration depth. Alternatively, and in an approximative fashion, it describes the density of itinerant quasiparticles in the normal state, derivable from the Drude weight in the optical conductivity.⁵¹ For the BFM scenario investigated here, such a Drude component arises from an Aslamazov-Larkin term in the conductivity of the itinerant electrons,⁴⁰ involving the Cooperons and is contained in the second term of the Cooperon propagator, Equation (12). In order to estimate the density n_p of those Cooperons which give rise to such a Drude component, we have to attribute it to just that contribution of the Cooperon propagator, i.e.,

$$n_p = \frac{1}{N\beta} \sum_{\mathbf{q}, \omega_m} \frac{1}{v^2} \Pi^2(\mathbf{q}, \omega_m) K(\mathbf{q}, \omega_m), \quad (13)$$

where the uncorrelated part $(1/v^2) \sum_{\mathbf{q}, \omega_m} \Pi(\mathbf{q}, \omega_m)$ has been subtracted out of the thermal average of the doubly occupied sites, given by $\langle c_\uparrow^\dagger c_\downarrow^\dagger c_\downarrow c_\uparrow \rangle$. In Table II we present the mass and concentration of Cooperons for different temperatures and doping rates corresponding to the well underdoped

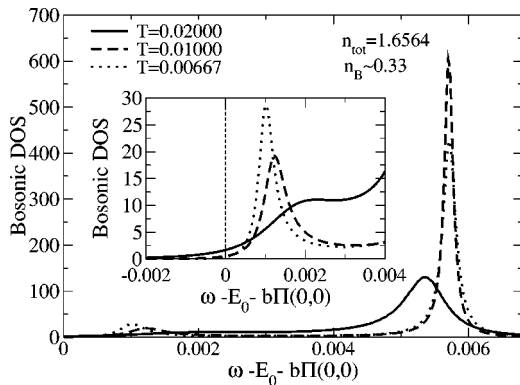


FIG. 9. Temperature evolution of the bosonic DOS for the underdoped regime with $n_{\text{tot}}=1.65$. The inset presents the low-energy part of this DOS.

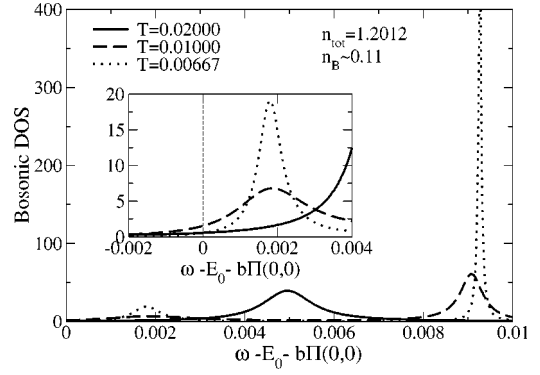


FIG. 10. Temperature evolution of the bosonic DOS for the underdoped regime with $n_{\text{tot}}=1.20$. The inset presents the low-energy part of this DOS.

($n_{\text{tot}} \approx 1.65$) and the less well underdoped ($n_{\text{tot}} \approx 1.20$) regime, for which the bosons have well defined propagating quasiparticle features.

In order to highlight the effect of the hard-core nature of the bosons we have repeated this study for the Cooperons for the case of normal bosons rather than hard-core bosons and present the corresponding values for the Cooperon mass and concentration by the numerical values, given in Table I, in the parenthesis.

The above assessment of the mass and concentration of the cooperons, contributing to the Drude peak in the normal state and ultimately to the superfluid current, shows that for hard-core bosons their concentration depends little on doping, while their mass depends on it sensibly. The latter rapidly increases, as, upon reducing the hole doping, we enter the regime of high boson concentration where correlation effects become increasingly important. As compared to the case of hard-core bosons, for normal bosons the variation with doping of the concentration of Cooperons turns out to be much more important, while for the mass it is less important. This leads, as we shall see below, to significant qualitative differences in the respective temperatures determining the onset of phase correlation driven superconductivity.

On the basis of these findings, we now attempt to estimate the critical temperature for phase fluctuation controlled superconductivity. For that we put $k_B T_\phi \approx \hbar^2 (n_p/m_p) a$, where n_p and m_p are our estimates for the density n_s and mass m_s of the superfluid charge carriers. a denotes a length scale

TABLE II. Variation of n_p , m_p , and n_F with temperature T for $n_{\text{tot}}=1.64$ (top) and $n_{\text{tot}}=1.20$ (bottom).

T	$n_p 10^3$	m_p	n_F
0.006 67	9.59	2.23	0.995
0.010 00	7.86	2.63	0.994
0.020 00	6.46	5.81	0.990
0.006 67	7.30	0.71	0.988
0.010 00	6.42	1.00	0.984
0.020 00	5.56	2.91	0.971

which is of the order of the coherence length or, alternatively, the interplane distance, depending on the degree of anisotropy of the system.

Assuming a in the expression for T_ϕ to be given by the lattice constant, corresponding to a layer compound system such as the HTSC, we trace this critical temperature as a function of doping (n_{tot} and $1 - n_F$) in Fig. 5. We notice a crossing of the energy scales related to the phase stiffness and to the electron pairing, as we approach the high doping limit, where the density of bosons is small and Cooperons are no longer well defined quasiparticles. This phase diagram, Fig. 5, corresponds to that proposed on the basis of the phase fluctuation scenario,¹⁶ but with the difference that there the doping dependent quantity of the phase stiffness was supposed to be related to the density of superfluid carriers, while, according to our present findings, based on the BFM scenario, it should be primarily related to the mass of the superfluid carriers—estimated as the mass of the Cooperons in our case. Upon approaching the optimally overdoped regime, where T_ϕ crosses T^* , the Cooperons loose their good quasiparticle features, and the onset of superconductivity is becoming controlled by amplitude fluctuations, as in a BCS system. The opposite trend with doping of T_ϕ and T^* , observed up to this level of doping, ceases accordingly and T_c is constraint to decrease, since being limited from above by the decreasing behavior of T^* which controls pair formation.

These features have been recently confirmed by an exact diagonalization study⁵² where for finite clusters the static correlation function $\langle \rho_{q=0}^+(t) \rho_{q=0}^-(t) \rangle$ has been studied for different boson concentrations n_B . It shows a characteristic temperature—strongly depending on n_B —where this correlation function shows a significant drop. This temperature can be used as an indication for the onset of long range phase pair correlations and hence can be compared with the T_ϕ in this paper. It shows a rapid increase with decreasing n_B and, upon approaching T^* , it smoothly follows that latter and decreases with further decreasing n_B .

In comparison to these features, derived by considering hard-core bosons, we find a noticeably different doping dependence of the phase fluctuation temperature when these hard-core effects are absent and the bosons are treated as normal bosons. See the corresponding values for T_ϕ^{NB} in Table I and its graphical representation in Fig. 5. T_ϕ^{NB} decreases much more moderately upon approaching the low doping regime, but both, T_ϕ^{NB} as well as T_ϕ converge to a finite value at $n_B = 0.5$. This is moreover again confirmed by this exact diagonalization study,⁵² showing a decrease and saturation of the static long wavelength phase correlation function upon increasing n_B and approaching its value 0.5.

In order to illustrate the combined effect of local electron pairing and phase correlations of those resonant pair states, we now examine the Cooperon propagator (12) in the low-frequency limit and interpret it in terms of its physically intuitive form, given in Eq. (2) in Sec. II. Let us for that purpose illustrate this Cooperon propagator in Fig. 11 as a function of temperature for two cases, representing a well underdoped and a less well underdoped situations, showing

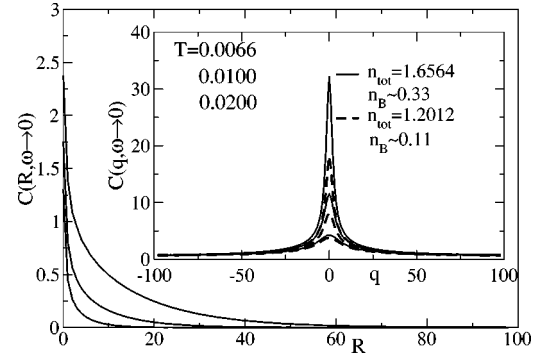


FIG. 11. Temperature evolution of the low-frequency limit of the Cooperon propagator in the underdoped regime with $n_{\text{tot}} = 1.65$ and $n_{\text{tot}} = 1.20$ (inset) and its spatial Fourier transform for $n_{\text{tot}} = 1.65$.

the tendency with increased hole doping. Fitting the spatial dependence of the Cooperon propagator to this phenomenological form, permits us to determine the various parameter which characterize it and which we enumerate in Table III. We notice that upon increasing the temperature, the coefficients C_a , weighting the short-range phase-uncorrelated local electron pairing, tend to rapidly decrease as we approach T^* in the entire doping regime. In the underdoped regime, upon decreasing the temperature and approaching T_ϕ , the coefficients C_ϕ , weighting the phase correlated electron pairs, increase rapidly together with the coherence length ξ , which is typically an order of magnitude bigger than the short-range electron-pair correlation length r_0 . In the optimally overdoped regime, on the contrary, C_ϕ hardly changes with temperature, while the coherence length follows the similar temperature dependence as in the underdoped regime. A systematic change is observed in the relative weight of the long-range to short-range contribution of the Cooperon correlation function C_ϕ/C_a , which, with increased hole doping, shows a decreasing behavior when evaluated for some characteristic doping dependent temperatures such as T^* . In particular, we find $C_\phi/C_a = 0.71, 0.45, 0.31$ for $n_{\text{tot}} = 1.65, 1.20, 1.02$ and corresponding values of $T^* \approx 0.016$,

TABLE III. Characteristic parameters of the Cooperon propagator (2) as a function of temperature T and for three doping rates $n_{\text{tot}} = 1.64$ (top), and $n_{\text{tot}} = 1.20$ (middle), and $n_{\text{tot}} = 1.02$ (bottom). ξ and r_0 are in units of the lattice constant a .

T	C_a	C_ϕ	r_0	$\xi(T)$
0.006 67	1.31	1.06	0.91	13.75
0.010 00	1.13	0.61	0.72	7.59
0.020 00	0.88	0.42	0.53	3.58
0.006 67	1.23	0.66	0.83	11.76
0.010 00	1.06	0.45	0.67	6.90
0.020 00	0.86	0.37	0.52	3.51
0.006 67	1.08	0.33	0.71	9.07
0.010 00	0.98	0.32	0.62	6.18
0.020 00	0.83	0.32	0.51	3.45

0.0142, 0.005 and $T_\phi=0.004, 0.010, 0.014$. It is this relative weight increase of amplitude versus phase contributions, as we go from the underdoped to the optimally overdoped regime, which indicates the change over from phase correlation driven superconductivity toward amplitude correlation driven superconductivity. A remarkable result is that neither the short nor the long-range scale depend sensitively on doping. We have some experimental indications^{53,54} from studies in the HTSC that, at least as far as ξ is concerned, its doping dependence is very weak.

VI. EVIDENCE FOR PAIRING CORRELATIONS IN THE SPECIFIC HEAT

The onset of the pseudogap, as seen in numerous experimental studies such as ARPES and single particle tunneling, indicate a loss of low energy single particle spectral weight. This loss of single particle spectral weight ought to be accompanied by a compensating increase of spectral weight coming from collective excitations, which, for the present precursor scenario, should predominantly come from pair fluctuations. Without having to go to elaborate spectroscopic techniques, indications for such many body effects are already seen in basic thermodynamic quantities such as the specific heat $C_V(T)$ and entropy $S(T)$, where a hump in C_V/T and a change in slope in $S(T)$ is observed at temperatures around T^* .⁵⁵ A recent theoretical approach⁵⁶ on the basis of a classical pair fluctuation scenario⁵⁷ attributed this hump feature very clearly to the contributions coming from pairing correlations, sitting on top of the single particle contributions.

We shall in this section present a similar investigation on the basis of the two-component precursor scenario adopted here. We evaluate for that purpose the inner energy, given by

$$\begin{aligned}
 U(T) &= E_{\text{kin}}^F(T) + E_{\text{kin}}^B(T) + E_{\text{int}}^{BF}(T) \\
 E_{\text{kin}}^F(T) &= \frac{1}{N} \sum_{\mathbf{k}} (\varepsilon_{\mathbf{k}} + \mu) n_{\mathbf{k}}^F(T) \\
 E_{\text{kin}}^B(T) &= \Delta_B n_B(T) \\
 E_{\text{int}}^{BF}(T) &= v \sum_i \langle (\rho_i^+ c_{i\downarrow} c_{i\uparrow} + \rho_i^- c_{i\uparrow}^+ c_{i\downarrow}^+) \rangle_T \\
 &= -\frac{2}{N\beta} \sum_{\mathbf{q}, \omega_m} \Pi(\mathbf{q}, \omega_m) K(\mathbf{q}, \omega_m) \quad (14)
 \end{aligned}$$

and subsequently determine $C_V(T) = (d/dT)U(T)$ and $S(T) = \int_0^T dT' C_V(T')/T'$. The fermion distribution function $n_{\mathbf{k}}^F(T)$, the number of bosons $n_B(T)$ and the expectation values of the interaction energy have to be calculated with respect to the full Hamiltonian. We illustrate in Fig. 12 the temperature variation of $C_V(T)$ and $S(T)$ for different total doping rates n_{tot} , corresponding to the underdoped situation and compare it with the noninteracting case ($v=0$) for the case of very small concentrations of bosons. The pseudogap is manifest in the diplike feature of $C_V(T)$ which occurs at T^* , together with a subsequent upturn of $C_V(T)$ upon low-

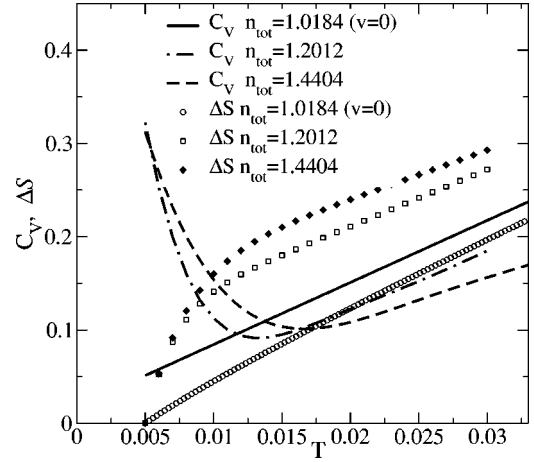


FIG. 12. Temperature evolution of the specific heat and entropy in the underdoped regime with $n_{\text{tot}}=1.44, 1.20$ and compared with the optimally overdoped regime $n_{\text{tot}}=1.02$.

ering the temperature which indicates the broad humplike structure above T_c . As we decrease n_{tot} upon going from the underdoped to the optimally overdoped regime, the dip moves to lower temperatures in agreement with a decreasing T^* and eventually disappears upon reaching a doping concentration where the number of bosons tends to zero (given approximately by the noninteracting BFM with $v=0$). At the same time the linear slope of $C_V(T)$ at high temperatures increases in correspondence with an increase of the DOS at the Fermi energy and saturating at the value characterizing the low boson concentration limit. Concerning the entropy, we are able to evaluate its increase $\Delta S(T)$ starting from a fixed lowest temperature and going up to the highest temperature we have been considering. The rapid rise in $\Delta S(T)$ below T^* , changing into a rather slow rise above T^* signals the existence of local order below T^* which gradually disappears when going beyond T^* to higher temperatures.

VII. SUMMARY

A doping induced change over from phase- to amplitude-fluctuation-driven superconductivity is shown to result in a system with precursor pairing within a two-component scenario, involving charge carriers with different statistics: fermions and bosons, coupled together via a charge exchange term. The fermions describe free electrons while the bosons (more precisely hard-core bosons) describe localized self-trapped electron pairs having spin- $\frac{1}{2}$ statistics which give rise to correlation effects in such a system. The opposite variation with doping of T^* and T_c is obtained, where the critical temperature is given by the phase stiffness of the system. With decreasing the concentration of the localized electron pairs, the energy associated with this phase stiffness crosses the pairing energy $k_B T^*$ in the itinerant electrons subsystem at a certain characteristic doping level. There, phase fluctuation controlled superconductivity changes over into amplitude fluctuation controlled superconductivity, giving rise to a phase diagram, which, qualitatively, is reminiscent of that proposed for the HTSC within the so-called phase fluctuation

scenario. The doping dependent length scales for short-range local electron-pair correlations and long-range phase correlations are discussed on the basis of the spectral properties of the Cooperon propagator, describing the exchange induced pairing in the electron subsystem. In the precursor pairing scenario studied here, it turns out that it is the degree of itinerancy of the Cooperons rather than their concentration which controls the doping dependence of the phase stiffness. This degree of itinerancy varies from well defined itinerant electron-pair states in the limit of high concentration of localized bound electron pairs (low hole doping) to overdamped excitations in the limit of low concentration of localized bound electron pairs (high hole doping).

The phase diagram, Fig. 5, represented as a function of doping, involves changes in the concentration of electrons away from half filling (hole doping) for given changes in total concentration of charge carriers n_{tot} . The variation of the hole doping [changes in $(1 - n_F)$ of the order of 2%] in this phase diagram is small compared to changes in n_{tot} , which is due to the 1D situation we have been considering here. This result is less surprising when we consider a 2D system with an anisotropic charge exchange coupling between the bound electron pairs and the bare itinerant electrons. One would then obtain a corresponding anisotropic

pseudogap, similar to what is observed in the HTSC. Hole doping would now affect roughly equally all the regions near the 2D Fermi surface, and thus attributing only a very small fraction of the doped holes to the actual regions in the Brillouin zone where the pseudogaps are formed, i.e., around the M points and along lines parallel to $[0,0]-[0,\pi]$ and equivalents.

One of the outstanding problems to be solved within such a precursor scenario for superconductivity is to understand how the transition to the superconducting state occurs. This involves a competition between Cooper pairing and real space pairing and necessitates a generalization of the present system of Green's functions by including the anomalous Green's functions in order to treat superconducting fluctuations. This problem will be the issue of future studies.

ACKNOWLEDGMENTS

The authors are extremely grateful to B. K. Chakraverty, M. Cuoco, T. Domanski, and G. Jackeli for innumerable discussions on this subject as well as for help in setting up the diagrammatic procedure for hard-core bosons, and for assistance with numerical procedures.

-
- ¹T. Timusk and B. Stratt, Rep. Prog. Phys. **62**, 61 (1999).
²J. Corson, R. Mallozzi, J. Orenstein, J. N. Eckstein, and I. Bozovic, Nature (London) **398**, 221 (1999).
³Z. A. Xu, N. P. Ong, T. Kakeshita, and S. Uchida, Nature (London) **406**, 486 (2000).
⁴I. Iguchi, T. Yamaguchi, and A. Sugimoto, Nature (London) **412**, 420 (2001).
⁵G. Deutscher, Nature (London) **397**, 410 (1999).
⁶H.-Y. Choi, Y. Bang, and D. K. Campbell, Phys. Rev. B **61**, 9748 (2000).
⁷C. C. Homes, T. Timusk, R. Liang, D. A. Bonn, and W. N. Hardy, Phys. Rev. Lett. **71**, 1645 (1993).
⁸D. N. Basov, C. C. Homes, E. J. Singley, M. Strongin, T. Timusk, G. Blumberg, and D. van der Marel, Phys. Rev. B **63**, 134514 (2001).
⁹C. Panagopoulos, J. R. Cooper, T. Xiang, Y. S. Wang, and C. W. Chu, Phys. Rev. B **61**, R3808 (2000).
¹⁰V. M. Krasnov, A. Yurgens, D. Winkler, P. Delsing, and T. Claesson, Phys. Rev. Lett. **84**, 5860 (2000).
¹¹M. Suzuki and T. Watanabe, Phys. Rev. Lett. **85**, 4787 (1991).
¹²M. Kugler, O. Fischer, C. Renner, S. Ono, and Y. Ando, Phys. Rev. Lett. **86**, 4911 (2001).
¹³Y. J. Uemura *et al.*, Phys. Rev. Lett. **62**, 2317 (1989).
¹⁴A. Sewer and H. Beck, Phys. Rev. B **64**, 224524 (2001).
¹⁵H. V. Kruis, I. Martin, and A. V. Balatsky, Phys. Rev. B **64**, 054501 (2001).
¹⁶V. J. Emery and S. A. Kivelson, Nature (London) **374**, 434 (1995).
¹⁷S. D. Palo, C. Castellani, C. D. Castro, and B. K. Chakraverty, Phys. Rev. B **60**, 564 (1999).
¹⁸B. K. Chakraverty, Physica C **341**, 75 (2000).
¹⁹M. Randeria, in *Bose Einstein Condensation*, edited by A. Griffin, D. Snoke, and S. Stringari (Cambridge University Press, Cambridge, UK, 1995), p. 434.
²⁰A. Y. Cherny and A. A. Shanenko, Phys. Rev. B **60**, 1276 (1999).
²¹M. R. Norman, H. Ding, J. C. Campuzano, T. Takeuchi, M. Randeria, T. Yokoya, T. Takahashi, T. Mochiku, and K. Kadowaki, Phys. Rev. Lett. **79**, 3506 (1997).
²²L. P. Kadanoff and P. C. Martin, Phys. Rev. **124**, 670 (1961).
²³O. Tchernyshyov, Phys. Rev. B **56**, 3372 (1997).
²⁴B. Giovannini and C. Berthod, Phys. Rev. B **63**, 144516 (2001).
²⁵R. Micnas, M. H. Pedersen, S. Schafroth, T. Schneider, J. J. Rodriguez-Nunez, and H. Beck, Phys. Rev. B **52**, 16 223 (1995).
²⁶K. Levin, Q. Chen, I. Kosztin, B. Janko, Y.-J. Kao, and A. Iyengar, cond-mat/0107275 (unpublished).
²⁷D. Rohe and W. Metzner, Phys. Rev. B **63**, 224509 (2001).
²⁸T. K. Kopec, Phys. Rev. B **65**, 054509 (2002).
²⁹S. Allen, H. Touchette, S. Moukouri, Y. M. Vilks, and A.-M. S. Tremblay, Phys. Rev. Lett. **83**, 4128 (1999).
³⁰B. Kyung, S. Allen, and A.-M. S. Tremblay, Phys. Rev. B **64**, 075116 (2001).
³¹J. Ranninger and A. Romano, Phys. Rev. B **66**, 094508 (2002).
³²J. Ranninger and S. Robaszkiewicz, Physica B **135**, 468 (1985).
³³A. Mysyrowicz, E. Benson, and E. Fortin, Phys. Rev. Lett. **77**, 896 (1996).
³⁴A. Schnell, G. Roepke, and P. Schuck, Phys. Rev. Lett. **83**, 1926 (1999).
³⁵E. Altman and A. Auerbach, Phys. Rev. B **65**, 104508 (2002).
³⁶T. Domanski, cond-mat/0302406, Phys. Rev. A (to be published).
³⁷V. A. Yurovski and A. Ben-Reuven, cond-mat/0205267, Phys. Rev. A (to be published 1 April 2003).

- ³⁸R. Friedberg, T. Lee, and H. K. Ren, *Phys. Rev. B* **50**, 10 190 (1994).
- ³⁹J. Ranninger, J.-M. Robin, and M. Eschrig, *Phys. Rev. Lett.* **74**, 4027 (1995).
- ⁴⁰P. Devillard and J. Ranninger, *Phys. Rev. Lett.* **84**, 5200 (2000).
- ⁴¹T. Domanski and J. Ranninger, *Phys. Rev. B* **63**, 134505 (2001).
- ⁴²J.-M. Robin, A. Romano, and J. Ranninger, *Phys. Rev. Lett.* **81**, 2755 (1998).
- ⁴³V. G. Vaks, S. A. Pikin, and A. Larkin, *Sov. Phys. JETP* **26**, 188 (1968).
- ⁴⁴Y. Izyumov and Y. Skryabin, *Statistical Mechanics of Magnetically Ordered Systems* (Consultant Bureau, New York, 1988).
- ⁴⁵H. Tolentino, F. Bandelet, A. Fontaine, T. Gourieux, G. Krill, J. Y. Henry, and J. Rossat-Mignod, *Physica C* **192**, 115 (1992).
- ⁴⁶A. A. Kordyuk, S. V. Borisenko, M. S. Golden, S. Legner, K. A. Nenkov, M. Knupfer, J. Fink, H. Berger, L. Forro, and R. Follath, *Phys. Rev. B* **66**, 014502 (2002).
- ⁴⁷M. Merz, N. Nuecker, P. Schweiss, S. Schuppler, C. T. Chen, V. Chakarian, J. Freeland, Y. U. Idzerda, M. Klaeser, G. Mueller-Vogt, and T. Wolf, *Phys. Rev. Lett.* **80**, 5192 (1998).
- ⁴⁸S. Lupi, P. Calvani, M. Capizzi, and P. Roy, *Phys. Rev. B* **62**, 12 418 (2000).
- ⁴⁹J. Ranninger and J.-M. Robin, *Physica C* **253**, 279 (1995).
- ⁵⁰N. M. Hugenholtz and D. Pines, *Phys. Rev.* **116**, 489 (1959).
- ⁵¹D. B. Tanner *et al.*, *Physica B* **244**, 1 (1998).
- ⁵²M. Cuoco, C. Noce, J. Ranninger, and A. Romano, *cond-mat/0305075*, *Phys. Rev. B* (to be published).
- ⁵³H. H. Wen, X. H. Chen, W. L. Yang, and Z. X. Zhao, *Phys. Rev. Lett.* **85**, 2805 (2000).
- ⁵⁴T. Shibauchi *et al.*, *Phys. Rev. Lett.* **86**, 5763 (2001).
- ⁵⁵J. W. Loram, J. Luo, J. Cooper, W. W. Liang, and J. L. Tallon, *Physica C* **341**, 831 (2000).
- ⁵⁶C. P. Moca and B. Janko, *Phys. Rev. B* **65**, 052503 (1995).
- ⁵⁷Y. M. Vilc and A. M. S. Tremblay, *J. Phys. I (France)* **7**, 1309 (1997).